Deuteron-nucleus elastic scattering: Solution of the standard model via the finite element method

R. Kozack*
Physics Department, Ohio State University, Columbus, Ohio 43210

F. S. Levin
Physics Department, Brown University, Providence, Rhode Island 02912
(Received 19 March 1987)

The standard, three-body model of deuteron-nucleus elastic scattering and breakup is described by a Hamiltonian consisting of the neutron and proton binding interaction and their kinetic energy operators, while the interaction of each nucleon with the (unexcited) target nucleus is represented by an absorptive, optical-type potential at fixed energy. The standard method for solving this model involves expanding the three-body wave function in states of the neutron-proton system and then truncating some or all of the continuum states in the expansion. Within such an approximation technique, it is not possible to determine the importance of (the neglected) high-lying continuum states. Their contribution can in principle be estimated, however, by employing a solution algorithm which avoids the eigenstate expansion technique. This is done in the present paper by means of the finite element method, applied to the solution in coordinate space. Two different models for the potentials were investigated: that of Farrell, Vincent, and Austern, in which all form factors are of Gaussian type; and a second in which Woods-Saxon form factors were used for the absorptive potentials. The only stable results obtained were for elastic S-matrix elements of the model of Farrell, Vincent, and Austern. These results were in good agreement with the elastic S-matirx elements S_L as calculated using an L^2 discretization ("variational") procedure and via the continuum, discretized, coupled-channels method, at an incident energy of 22.9 MeV. This agreement confirms that neglect of the high-lying, neutron-proton continuum states is a valid approximation for determining elastic S-matrix elements. The persistent instability of the numerically determined, finite-element-method elastic S_L's for the Woods-Saxon case and of the breakup S-matrix elements is an example of the inappropriate application of the asymptotic boundary conditions, recently discussed by Kuruoglu and Levin.

I. INTRODUCTION

It is standard practice to describe deuteron-nucleus elastic scattering and elastic breakup—the processes A(d,d)A and A(d,np)A—in terms of a three-body model. Most numerical analyses are based on an effective Hamiltonian of the form[1]

$$H_M = K_R + K_{np} + V_{np} + \mathcal{V}_n + \mathcal{V}_p , \qquad (1.1)$$

where K_R is the kinetic energy operator for the relative motion between the deuteron center of mass and the target center of mass, K_{np} is the kinetic energy operator for the relative motion between the neutron and proton, V_{np} is the neutron-proton interaction which binds the deuteron, and $\mathcal{V}_n$ ($\mathcal{V}_p$) is usually assumed to be the neutron-nucleus (proton-nucleus) optical potential evaluated at an energy $E_d/2$, where $E_d = E - \epsilon_d - \epsilon_0$, with $\epsilon_d(\epsilon_0)$ the deuteron (target nucleus) binding energy.

H_M is an approximation to the three-body Hamiltonian H_3 which provides an exact description of the two elastic processes (d,d) and (d,np). In a recent paper[2] we have shown that the general form taken by H_3 is

$$H_3 = K_R + K_{np} + V_{np} + \mathcal{V}_n^{opt}(E - \epsilon_0 - K_p)$$
$$+ \mathcal{V}_p^{opt}(E - \epsilon_0 - K_n) + W_{np} , \qquad (1.2)$$

which is the form originally inferred by Austern and Richards.[3] Here, $\mathcal{V}_n^{opt}$ ($\mathcal{V}_p^{opt}$) is the antisymmetrized complex ("optical") potential well describing neutron-nucleus (proton-nucleus) elastic scattering but evaluated at the shifted "energy" $E - \epsilon_0 - K_p$($E - \epsilon_0 - K_n$), where ϵ_0 is the target nucleus ground state energy and K_p (K_n) is the kinetic energy operator for the spectator proton (neutron). The quantity W_{np} is an effective three-body interaction. Although W_{np} is too complicated to evaluate exactly, we have been able to show that it contains no terms which, when combined with the V_{np} term in (1.2), ultimately yields an interaction of the form QV_{np} or $V_{np}Q$, where Q is a Pauli-blocking operator.[4]

To go from (1.2) to (1.1) requires two approximations, viz., that W_{np} be neglected and that the energy dependence $E - \epsilon_0 - K_i$, $i = $n or p, be replaced by $E_d/2$. The former approximation will be valid if W_{np} is small; the latter has been argued, on the one hand, to result from a "suitable" averaging process[3] and on the other to be valid if the neutron and the proton in the (d,np) process are each

detected at scattering angles that are not too large.[5] We note that the $E-\epsilon_0-K_i\rightarrow E_d/2$ replacement changes the basic physics associated with the $H_{A+2}\rightarrow H_3$ reduction. That is, H_3 not only describes deuteron elastic scattering and elastic breakup, it also describes those neutron and proton stripping processes in which the target ground state is the only parent for the residual nuclear state (see the Appendix for further comments on this). H_M, on the other hand, by forcing the energy dependence of $\mathcal{V}_n^{opt}$ and $\mathcal{V}_p^{opt}$ to be a positive constant, does not allow for flux going into stripping channels (i.e., for rearrangement): it is a model for elastic scattering and breakup only. This follows from the fact that a complex potential cannot in general produce a particle-stable state.

Because of the above limitation, H_M defines a special three-body model, viz., one in which the solution can be obtained without use of the Faddeev equations,[6] as we show in the Appendix. Even with this simplification, the fact that one is still dealing with a three-body problem means that numerical solutions remain nontrivial to obtain since the Schrödinger equation involves two vector variables, rather than one (as in a two-body problem).

A variety of approximations have been used previously to obtain elastic and breakup amplitudes for the H_M problem. These approximations can be generally characterized as reducing the three-body problem of Eq. (1.1) to a set of effective, two-body, coupled-channel equations. This is typically done by first employing the eigenstates of the internal deuteron Hamiltonian $H_{np}=K_{np}+V_{np}$ as an expansion basis for the model wave function ψ_M. These eigenstates obey

$$H_{np}\begin{Bmatrix}\phi_d(\mathbf{r})\\\phi_k^{(\pm)}(\mathbf{r})\end{Bmatrix}=\begin{Bmatrix}\epsilon_d\phi_d(\mathbf{r})\\\epsilon_k\phi_k^{(\pm)}(\mathbf{r})\end{Bmatrix}, \tag{1.3}$$

where ϕ_d is the deuteron bound state with binding energy ϵ_d, while $\{\phi_k^{(\pm)}\}$ is the set of neutron-proton continuum states whose energies are $\epsilon_k=\hbar^2k^2/M$, and $\mathbf{r}$ is the neutron-proton relative separation. The relevant expansion is then

$$\psi_M(\mathbf{r},\mathbf{R})=\phi_d(\mathbf{r})\mathcal{X}_d(\mathbf{R})+\int d^3k\,\phi_k^{(+)}(\mathbf{r})\mathcal{X}_k(\mathbf{R})$$

$$\equiv P\psi_M(\mathbf{r},\mathbf{R})+Q\psi_M(\mathbf{r},\mathbf{R}), \tag{1.4}$$

where $P+Q=1$, P projects onto ϕ_d, and $\mathbf{R}$ is the deuteron c.m. coordinate. The scattering coefficients $\mathcal{X}_d$ and $\mathcal{X}_k$ yield, respectively, the elastic scattering amplitude and the breakup amplitude associated with a n-p relative motion state of momentum $\mathbf{k}$.

Substitution of (1.4) into

$$(E-\epsilon_0-H_M)\psi_M=0, \tag{1.5}$$

followed by projection onto ϕ_d and $\phi_k^{(+)}$ yields an infinite set of coupled equations for the $\mathcal{X}$'s. They are solved in practice by one or another truncation/discretization approximation. The simplest approximation is to assume $Q\psi_M=0$, which leads to the Watanabe (WAT) or folding model.[7] The Watanabe model totally neglects breakup and therefore underestimates absorption from the elastic

channel. The next simplest method is to assume that only lower-energy continuum states are important in Eq. (1.5) and that their energy can be set equal to the deuteron binding energy. This approximation is known as the adiabatic (AD) or Johnson-Soper model[8,9] and results in a one-variable equation in $\mathbf{R}$ in which r appears as a parameter.

More sophisticated approximation techniques involve replacing the single equation (1.5) by a set of coupled equations in $\mathbf{R}$. In one, known as the variational (VAR) method,[10] the deuteron continuum is replaced by a discrete set of L^2 basis functions, with the deuteron Hamiltonian H_{np} being diagonalized within this limited set. In the most sophisticated one, the integral over $\mathbf{k}$ in Eq. (1.4) is given a finite cutoff and then broken up into intervals (bins), with an "average" wave function being computed for each interval.[11,12] This method is referred to as the continuum discretized coupled channels (CDCC) method. Convergence of the CDCC method with respect to variation of the cutoff and the width of the bins has been studied and obtained.[13] In addition, test calculations have shown that the CDCC and VAR methods give similar results,[9] and that the AD model agrees with them for incident deuteron energies above about 40 MeV.

Although the above results increase one's confidence in the CDCC and VAR approaches, these methods are unable to assess the contribution from the neglected set of high momentum components in the relative n-p motion. It is thus desirable to test these approaches against a method which does not employ low momentum approximations to the integral in Eq. (1.4). We have used such a method in our numerical study of the H_M model, results of which are reported in this article. The procedure we use is known as the finite element method.[14,15] In contrast to the expansions of Eqs. (1.3) and (1.4), the present application of this method involves the reduction of the infinite volume of the $\mathbf{r},\mathbf{R}$ coordinate space to a finite size, followed by discretization of this finite domain into subdomains or elements, and then finally an expansion of ψ_M via interpolation polynomials defined over one or at most a few elements. The scattering boundary conditions are imposed at the outer edges of the domain.

We describe this alternate procedure in Sec. II, while in Sec. III we give a brief description of the boundary conditions and of our choices for H_M. Pertinent details of our calculation are discussed in Sec. IV and our results and their comparison with those from the other methods, noted in the preceding, are presented in Sec. V. A stability analysis is given in Sec. VI and a summary is given in Sec. VII. The paper concludes with an Appendix on the general behavior and description of the H_M problem.

II. THE FINITE ELEMENT METHOD

The first successful use of a configuration space approach to solve nuclear three-body problems was that of Merkuriev, Gignoux, and Laverne, who employed a finite difference method.[16] More recently, Payne, Friar, Gibson,

and collaborators[17] have carried out position-space analyses of the three-nucleon system using the method of orthogonal collocation.[15] As noted above, our procedure for determining numerical solutions to the three-body H_M problem employs the finite element method (FEM), which is closely related to the orthogonal collocation method. In recent years, the finite element method has been applied to a variety of bound-state and collision systems in chemistry and physics, selected references to which can be found in Refs. 18–21.

For simplicity we describe the FEM in one dimension, as the generalization to higher dimensions is straightforward. To begin with, the line segment $[x_0, x_N]$ is divided into a mesh $\{x_0, x_1, \ldots, x_N\}$. These x_i's do not have to be placed at regularly spaced intervals and, indeed, a higher concentration of mesh points is normally used in regions where the wave function is expected to vary most. Once the mesh has been established a local basis function w_i is defined at each mesh point. The function w_i is called local because it is nonzero only in the interval $[x_{i-1}, x_{i+1}]$. For the present study, we have chosen the w_i's to be piecewise Hermite cubic polynomials.[15] The wave function is then expanded in terms of the basis functions as

$$\psi \approx \sum_j c_j w_j(x) . \tag{2.1}$$

(For this choice of w_i, the derivative of ψ is also expanded in cubic Hermites.) If the original equation is of the form $(H - E)\psi(x) = 0$, use of the expansion (2.1) leads to the approximate equation

$$(H - E) \sum_j c_j w_j(x) = 0 . \tag{2.2}$$

In the FEM, the scalar product of both sides of Eq. (2.2) is formed for each basis function, resulting in the matrix equation

$$\sum_j \int dx\, w_i(x)(H - E)w_j(x)c_j \equiv \sum_j A_{ij}c_j = 0 . \tag{2.3}$$

Once the behavior of ψ at x_0 and x_N has been specified, standard matrix techniques can be used to solve Eq. (2.3) for the unknown c_j's. If only local operators occur in (2.3), most of the matrix elements A_{ij} are zero (such a matrix is called "banded"). This results in a substantial savings of computer resources. For a two-dimensional problem, the only modification in the preceding analysis would be to expand ψ as

$$\psi = \sum_{ij} c_{ij} w_i(x)w_j(y) ; \tag{2.4}$$

the rest of the procedure goes through as before.

The utility of the FEM has been well established as a practical method for solving partial differential equations. In addition, the FEM has the virtue of being "numerically exact," i.e., it has been proved that the FEM solution converges to the true solution as more and more points are added to the mesh.[14]

III. H_M MODELS AND BOUNDARY CONDITIONS

In order to compare our results with those of other calculations, we must use the same potentials V_{np}, $\mathcal{V}_n$, and $\mathcal{V}_p$ as employed in these calculations. For V_{np} this means assuming that it carries an angular momentum projection operator which restricts the n-p relative motion states to S waves $(l = 0)$ only. This assumption, plus the short-range nature of $\mathcal{V}_n$ and $\mathcal{V}_p$, allows for a straightforward determination of the asymptotic boundary conditions to be imposed on $\psi_M(\mathbf{r}, \mathbf{R})$ and we examine this point first.

The lack of spin and the $l = 0$ behavior of the n-p motion means that $\psi_M(\mathbf{r}, \mathbf{R}) \rightarrow \psi_M(r, \mathbf{R})$. Hence, the partial wave expansion of ψ_M is

$$\psi(r, \mathbf{R}) = \sum_L \frac{u_L(r, R)}{rR} Y_{L0}(\theta_R, \varphi_R) , \tag{3.1}$$

which yields a set of uncoupled equations in the two scalar variables r and R.

The effective Schrödinger equation that u_L obeys is

$$\left[-\frac{\hbar^2}{M} \left[\frac{\partial^2}{\partial r^2} + \frac{1}{4} \frac{\partial^2}{\partial R^2} + \frac{L(L+1)}{R^2} \right] \right.$$
$$\left. + V_{np}(r) + \overline{U}(r, R) - E \right] u_L(r, R) = 0 , \tag{3.2}$$

where we have set $\epsilon_0 = 0$ and

$$\overline{U}(r, R) = \frac{1}{4\pi} \int d\Omega_r [\mathcal{V}_n(|\mathbf{R} + \tfrac{1}{2}\mathbf{r}|) + \mathcal{V}_p(|\mathbf{R} - \tfrac{1}{2}\mathbf{r}|)] . \tag{3.3}$$

It is convenient to change from the rectangular coordinates (r, R) to hyperspherical ones (ρ, θ), defined by

$$r = \rho \cos\theta , \tag{3.4}$$

$$R = \tfrac{1}{2}\rho \sin\theta . \tag{3.5}$$

Thus, $u_L(r, R) \rightarrow u_L(\rho, \theta)$, and the appropriate boundary conditions are that u_L vanish for $\rho = 0$ and $\theta = 0$ and $\pi/2$, while as ρ approaches infinity we assume that u_L behaves as

$$u_L(\rho, \theta) \underset{\rho \to \infty}{\sim} \phi_d(\rho \cos\theta)[\hat{j}_L(Q\rho \sin\theta/2)$$
$$+ A_L \hat{h}_L^{(+)}(Q\rho \sin\theta/2)]$$
$$+ a_L(\theta)e^{i\sqrt{E}\rho}/\rho^{1/2} , \tag{3.6}$$

where Q is the momentum of the incident deuteron, E is the total energy, $\hat{j}_L$ and $\hat{h}_L^{(+)}$ are the Ricatti-Bessel and outgoing-wave Ricatti-Hankel functions,[22] respectively, and we have now shifted to units in which $\hbar = M = 1$.

The $\phi_d[\ ]$ term on the right-hand side (rhs) of (3.6) refers to the incident wave and the elastically scattered one, while the term with $\rho^{-1/2}$ is associated with breakup. It is obvious that the ϕ_d portion of (3.6) will be nonnegligible only for those θ very close to $\pi/2$. Hence, at large ρ, most of the ρ, θ domain contains only breakup

contributions. The combining in (3.6) of the elastic and the breakup parts of the asymptotic boundary conditions follows the work of Ref. 16. Note that the elastic scattering amplitude can be determined from the A_L's. In practice, of course, both ρ and L must be truncated. The accuracy of such truncations is discussed below.

The detailed forms of the potentials remain to be specified. For V_{np} we have used the Gaussian form

$$V_{np}(r) = -V_0 e^{-\beta r^2} , \qquad (3.7)$$

with $V_0 = 66.99$ MeV and $\beta = 0.415$ fm^{-2}, which yields a deuteron binding energy of 2.22 MeV.

Two forms for the optical potentials have been used in our calculations. In one, known as the Farrell-Vincent-Austern model,[11] $\mathcal{V}_n(x_n)$ and $\mathcal{V}_p(x_p)$ were chosen to have the same Gaussian functional form, viz.,

$$\mathcal{V}_n(x) = \mathcal{V}_p(x) = -U_0 e^{-\alpha x^2} , \qquad (3.8)$$

where $U_0 = (50 + 5i)$ MeV and $\alpha = 0.0625$ fm^{-2}. In addition to ignoring spins and Coulomb effects, and requiring $l = 0$ neutron-proton states, this model also assumes that the target nucleus is infinitely heavy. This is an important three-body model because it has been studied by all of the approximation techniques described in Sec. I. It is this model for which we present results of our FEM calculations.

In the second choice for $\mathcal{V}_n$ and $\mathcal{V}_p$, the Gaussian $\exp(-\alpha r^2)$ of (3.8) was replaced by a Woods-Saxon form, viz., $\{1 + \exp[(x - x_0)/a]\}^{-1}$. This latter choice led to major problems, as discussed below, and no results based on it are given here.

Finally, the incident deuteron energy was chosen as 22.9 MeV,[9,11] corresponding to a total energy of 20.68 MeV. The value $\hbar^2/M = 41.47$ MeV fm^2 was used, where M is the nucleon mass.

IV. DETAILS OF THE FEM CALCULATIONS

Before presenting our results, we first discuss some details of the FEM calculation. We tested this numerical procedure by applying it to the case of three identical particles,[23] for which published results exist.[16,17,24] The experience gained in securing agreement with these latter results was helpful in carrying out the deuteron-nucleus FEM computations.

Separate procedures were used for specifying the meshes in the ρ and θ variables. The ρ direction was divided into two regions. In the inner region, including the origin, the mesh was given by the formula

$$\rho_i = \frac{A_\rho^i - 1}{A_\rho^{N_\rho} - 1} \rho_{max} , \qquad (4.1)$$

where A_ρ is the meshing parameter which determines the relative density of mesh points near the origin, N_ρ is a number of points, and ρ_{max} is the point where the first region ends. In the present calculations, $A_\rho = 1.01$, $N_\rho = 45$, and $\rho_{max} = 20.0$ fermis. In the outer region, beyond 20 fermis, the mesh points were equally spaced at

intervals of 5/6 fermis. Obviously, as the bombarding energy increases, more and more mesh points must be added to reproduce the proper oscillatory behavior of the wave function. The final cutoff value for ρ was determined by checking the stability of the results as the cutoff value was increased. In our calculation, a final cutoff value of 30 fermis was found to be sufficient for the FVA model, making a total of 57 points in the ρ direction.

In the θ direction, the mesh was laid out according to the formula

$$\theta_i = \frac{\pi}{2} - \frac{\pi}{2} \frac{A_\theta^i - 1}{A_\theta^{N_\theta} - 1} , \qquad (4.2)$$

where $A_\theta = 1.23$ and $N_\theta = 16$. The form of Eq. (4.2) ensures that a higher density of mesh points occurs near $\theta = \pi/2$, where the potential V_{np} is strongest. The meshing parameter A_θ must be sufficiently large to accurately reproduce the deuteron wave function at large values of ρ.

To recover the physical scattering amplitudes from the FEM calculation, either of two procedures can be followed, viz., either the asymptotic form of the FEM solution can be compared with the asymptotic form (3.6), or the complete FEM solution (over the truncated space) can be used to calculate the integral form of the appropriate amplitude. For example, in an r,R representation, the integral expression for the elastic amplitude is given by

$$A_L = -\frac{4M(-i)^L}{\hbar^2 Q} \int_0^\infty \int_0^\infty dr \, dR \, \hat{j}_L(QR) \phi_d(r)$$

$$\times \overline{U}(r,R) u_L(r,R) . \qquad (4.3)$$

In our FVA-model calculations of A_L, the integral form (4.3) gave far more stable results with respect to variation of the cutoff value of ρ than did extraction from the asymptotic form. Therefore, all of the results given in the following section were obtained from use of Eq. (4.3). For the FVA-model breakup amplitude, neither comparison with the asymptotic form (3.6) nor a calculation of the integral form of the breakup amplitude gave stable results. Hence, there are no breakup results for the FVA model presented in the next section. In the case of the Woods-Saxon form-factor calculations, neither the asymptotic form nor the integral representation led to any stable results: Both A_L and $a_L(\theta)$ were sufficiently unstable, even for a ρ cutoff of 65 fm, that no results for this case are listed in Sec. V. These various instabilities are discussed in Sec. VI. However, we emphasize that the A_L for the FVA model were sufficiently stable when calculated via the matrix element method to be reliable, and as such, are listed in the next section.

V. NUMERICAL RESULTS

We have calculated the elastic S-matrix elements for the FVA deuteron-nucleus model described in Sec. III. This model was originally studied by Farrell, Vincent, and Austern[11] using both the CDCC and WAT methods. The

FVA model was also investigated by Amakawa, Mori, Nishioka, Yazaki, and Yamaji[9] within the VAR and AD approximations. We will compare our FEM results with those obtained in Refs. 9 and 11.

Although each of the above studies used the same nucleon-nucleus absorptive potentials, there were differences in the choice of V_{np}. Farrell, Vincent, and Austern worked solely in terms of a set of deuteron eigenstates, and since the continuum states were not orthogonal to the bound state, it is not possible to infer a form for V_{np}. In the VAR calculation, a "soft-core" potential, given by a sum of Gaussians, was employed.[9] On the other hand, a Yamaguchi separable potential[25] was used for the AD calculation.[9] While a separable potential is a convenient way to generate a set of deuteron eigenstates, it would be more difficult to use it in a FEM calculation, since its nonlocality would destroy the bandedness property of the matrix A_{ij} given in Eq. (2.3). As noted earlier, a simple one-term Gaussian form for V_{np} was used in the present calculation. It will be shown below that the FEM deuteron-nucleus elastic scattering observables are relatively insensitive to the choice of V_{np}, thereby making a comparison between the different studies meaningful.

We have chosen to present our results in terms of phase shifts (δ_L) and absorption coefficients (η_L). These quantities are related to A_L by

$$A_L = \frac{\eta_L e^{2i\delta_L} - 1}{2i} \equiv \frac{S_L - 1}{2i} .$$ (5.1)

The FEM results together with those obtained with the CDCC, VAR, AD, and WAT methods are given in Tables I and II. (The numerical values of S_L for these other methods have been estimated from the Argand diagrams in Refs. 9 and 11.) As can be seen, the largest differences occur for $L \leq 3$, although all of the calculations are qualitatively similar for these values of L. For $4 \leq L \leq 8$, the FEM, CDCC, and VAR give quite similar results. This might have been anticipated, since the

TABLE I. Phase shifts δ_L for elastic deuteron scattering at 22.9 MeV.

L	FEM	CDCC	VAR	AD	WAT
0	69	74	64	65	50
1	59	68	65	60	45
2	48	55	47	46	34
3	31	53	38	29	16
4	9	12	7	4	−6
5	−19	−19	−17	−27	−36
6	−58	−58	−65	−66	−72
7	66	72	66	68	64
8	11	12	9	14	14
9	−45	−46	−48	−45	−48
10	70	72	72	67	69
11	34	34	35	31	34
12	17	17	18	14	17
13	8	9	9	9	8
14	4	4	4	4	4
15	2			2	2

TABLE II. Inelasticities η_L for elastic deuteron scattering at 22.9 MeV.

L	FEM	CDCC	VAR	AD	WAT
0	0.16	0.22	0.21	0.18	0.30
1	0.18	0.22	0.18	0.19	0.31
2	0.21	0.22	0.22	0.21	0.32
3	0.22	0.23	0.22	0.21	0.30
4	0.24	0.23	0.22	0.22	0.33
5	0.23	0.24	0.25	0.22	0.34
6	0.20	0.22	0.18	0.25	0.35
7	0.21	0.19	0.19	0.27	0.36
8	0.33	0.31	0.33	0.35	0.37
9	0.42	0.42	0.42	0.41	0.42
10	0.53	0.57	0.55	0.55	0.61
11	0.74	0.75	0.77	0.77	0.82
12	0.89	0.88	0.89	0.89	0.93
13	0.94	0.94	0.94	0.96	0.97
14	0.97	0.98	0.98	0.98	0.98
15	0.99			0.99	0.99

CDCC and VAR methods are expected[9] to be the most accurate techniques of those which have been previously used to study deuteron-nucleus scattering. Next best in the $4 \leq L \leq 8$ range are the AD results, followed by the WAT calculation. Above $L = 8$, all five methods agree very well with each other. The convergence of our calculations is demonstrated by the fact that the δ_L's rapidly approach zero at the same time that the η_L's approach unity. Thus, as usual, this behavior justifies the truncation of the calculation with respect to L.

To see how the above-mentioned differences affect the elastic scattering observables, the contribution to scattering from all partial waves must be summed. Because of the factor of $2L + 1$ that occurs in the sums for the various cross sections, the lowest L values make relatively small contributions and therefore one would not expect large differences between the FEM, CDCC, and VAR results for elastic scattering observables. This is borne out by Fig. 1, which compares the differential cross sections obtained with the FEM, CDCC, and VAR methods. As can be seen, the major differences occur in the minimum near 60° and at backangles. Differences between either the CDCC or the VAR calculations and the FEM calculation are, in general, no greater than those between the CDCC and VAR calculations themselves. The FEM, AD, and WAT differential cross sections are shown in Fig. 2. As expected, the AD result is better than the WAT result, but not as good as the CDCC and VAR results. The total, elastic, and absorption cross sections for all five methods are given in Table III.

The good agreement of the FEM calculations with both the CCDC and VAR results leads us to conclude that each of the latter methods is reliable for obtaining elastic cross sections. Amakawa et al. have already reached this conclusion[9] based on a comparison of the CDCC and VAR methods. Our confirmation of this conclusion is based on an independent method that does not rely on an expansion of the three-body wave function in terms of a global basis
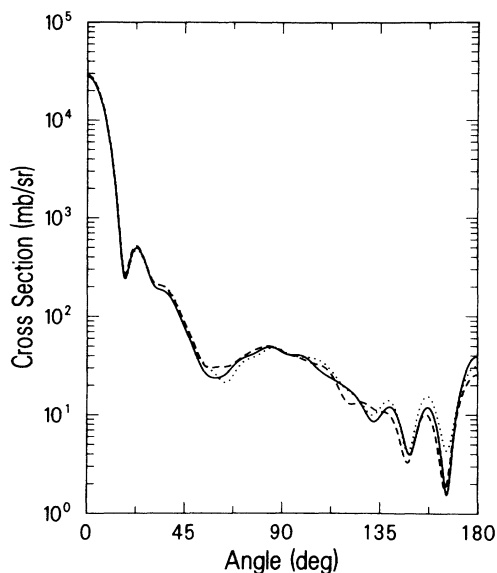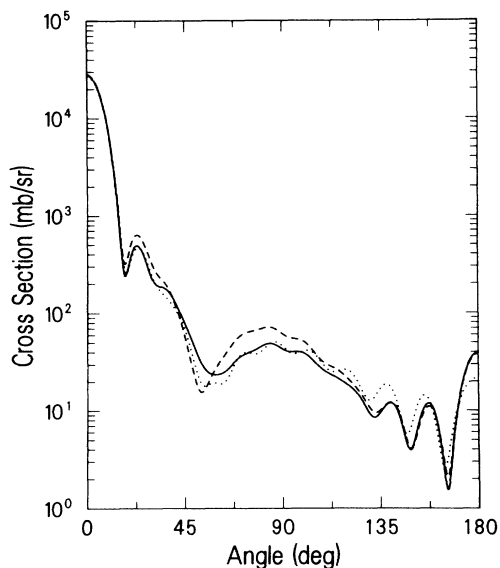
FIG. 1. Elastic differential cross sections for the FVA model calculated by three different methods. The solid line is the FEM calculation, the dotted line is the CDCC result, and the dashed line is the VAR computation.

set followed by neglect of high momentum components.

Finally, we comment on the sensitivity of our calculation to the choice of V_{np}. As stated earlier, although each of the calculations for which we have made comparisons used the same model for $\mathcal{V}_n$ and $\mathcal{V}_p$, they differed in their treatment of V_{np}. The sensitivity of the FEM solution to V_{np} was tested by comparing three sets

FIG. 2. Elastic differential cross sections for the FVA model calculated by three different methods. The solid line is the FEM calculation, the dotted line is the AD result, and the dashed line is the WAT computation.

TABLE III. Comparison of deuteron cross sections in fm^2 at $E_d = 22.9$ MeV.

	σ_{el}	σ_{ab}	σ_{tot}
FEM	246	182	428
CDCC	260	180	440
VAR	257	179	436
AD	246	177	423
WAT	267	163	430

of calculations, each with a different V_{np}. In addition to the Gaussian potential, the soft-core "sum of Gaussians" potential of Ref. 9, and the Hulthén-type potential considered by Anders and Linder,[10] was used. The phase shifts and absorption parameters for each potential for the values $0 \leq L \leq 3$ are presented in Table IV. Although each potential yields the same deuteron binding energy, they give different values for δ_L and η_L at low L. Above $L = 3$, all the phase shifts agree with those in the first column of Table I to within 1° (except for an isolated case where one phase shift differs by 3°), and all the absorption parameters are within 0.01 of those given in the first column of Table II. The three potentials, of course, give slightly different cross sections, but the differences, shown in Fig. 3, are barely visible on the scale of the graph presented. Thus the fact that other V_{np}'s were used in the various calculations does not alter the conclusions of this paper, although clearly if one is making a detailed comparison for low L values, where the largest discrepancies between different methods occur, the same V_{np} must be used in each calculation.

VI. INSTABILITIES

Results have been presented only for the FVA elastic S-matrix elements S_L. Neither the FVA $a_L(\theta)$ nor the S_L and $a_L(\theta)$ values for the Woods-Saxon model were sufficiently stable with respect to changes in ρ (i.e., variations $\leq 2\%$) that we could rely on them. And, of the two methods of determining S_L, viz., from the asymptotic behavior of u_L and from the integral expression, only the latter led to stability in the FVA case: use of the former did not. As it turns out, the instabilities encountered for the H_M model at energies above the deuteron breakup threshold have also been encountered in configuration-space calculations of neutron-deuteron scattering and breakup: unpublished computations of Payne and collaborators[26] and of the present authors, each using a hyperspherical coordinate system, have failed to yield stable A_L and $a_L(\theta)$ at energies $E > |\epsilon_d|$.[27] Thus, there are two questions to be answered: Why do these instabilities occur, and why are our matrix element computations of A_L for the FVA model sufficiently stable to be reliable?

The occurrence of instabilities in position space breakup calculations using hyperspherical coordinates— of which the present computations as well as the unpublished ones of Payne and collaborators and of the present authors are all examples—are almost certainly due to the

TABLE IV. Comparison of S_L and η_L for different V_{np} at $E_d = 22.9$ MeV.

| | | δ_L | | | η_L | |
L	Gauss	Soft core	Hulthén	Gauss	Soft core	Hulthén
0	69	67	66	0.16	0.15	0.15
1	59	58	56	0.18	0.19	0.18
2	48	46	45	0.21	0.22	0.21
3	31	30	29	0.22	0.24	0.23

maximum values of ρ used in these computations not yet being in the asymptotic region. As a consequence, the asymptotic form (3.6), though imposed on the numerical solution, is not a valid representation of u_L at the maximum ρ values used in the computations. Since the form (3.6) is derived[28] from the stationary phase approximation,[29] the failure of the asymptotic form is actually due to invalid use of the stationary phase approximation. This latter conclusion is discussed by Kuruoglu and Levin,[30] who give specific examples of the errors that can arise in this situation, including an example in which an error of 25% at $\rho \cong 8300$ fm ($E \sim 20$ MeV) was found. The physical reason underlying the need to use extremely large values of ρ before applying (3.6) is[31] the long-range rescattering effect due to final state interactions.[32]

The above remarks account for the instabilities, but do not explain the stability of the FVA values of S_L as computed from the elastic matrix element. Our explanation of this is based on the fact that the optical potentials in the FVA case, due to their Gaussian form factors, are very short ranged, much more so than are the Woods-Saxon form factors in the other optical potential case. Now in the elastic matrix element, the integral contains the product

$$\phi_d(r)[\mathcal{V}_n(|\mathbf{R} + \tfrac{1}{2}\mathbf{r}|) + \mathcal{V}_p(|\mathbf{R} - \tfrac{1}{2}\mathbf{r}|)] .$$

Since $\phi_d(r)$ is the bound state solution to a short-ranged Gaussian potential, a nonzero integrand occurs only for small r. On the other hand, $\mathcal{V}_n$ ($\mathcal{V}_p$) also being short ranged means that in the integrand, the range of R cannot be very large. Hence, in the matrix element, $\psi(\mathbf{r}, \mathbf{R})$ is not needed for large values of r or R, so that its asymptotic form is not a crucial component, as long as the overall normalization of ψ is reasonably well determined. This is, of course, an old argument. It is significant in the present context because the uncertainties in the asymptotic form of u_L for the FVA case are smaller than for the Woods-Saxon case. As a result of the shorter range of the optical potentials in the former compared to the latter case, the asymptotic uncertainty plays a smaller role in the former case, leading to uncertainties in the matrix element form of S_L of the order of a few percent for the FVA model compared to about 10% for the Woods-Saxon form of S_L, even when calculated via the integral form.

VII. SUMMARY

In this paper we have presented results of a numerical study of the three-body deuteron-nucleus model using a method which does not, a priori, ignore large values of the neutron-proton relative momentum. Whereas previous methods of solution involve reducing the model to an effective one-body, coupled-channels (CC) problem, we have solved the full three-body problem using the finite element method (FEM). Although we have been unable to obtain stable results for breakup amplitudes (for reasons described in the foregoing), we have calculated elastic scattering S-matrix elements for the Farrell-Vincent-Austern model and have compared the results with those obtained by previously used techniques. For the lower partial waves, the FEM calculation gave qualitatively different results than the other approximation methods. Above $L = 3$, however, the FEM, CDCC, and the L^2-discretization (or VAR) methods all agreed well with each other, and yielded very similar differential cross sections as well. Thus, we have provided an independent test of the accuracy of the standard methods for calculating deuteron-nucleus elastic scattering parameters.
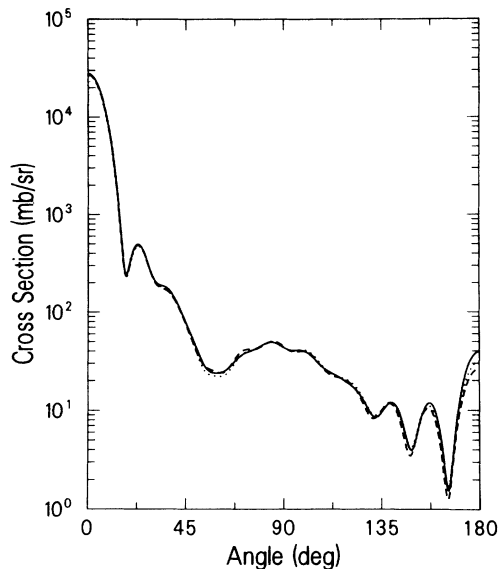
FIG. 3. Elastic differential cross sections for the FVA model calculated with different neutron-proton potentials V_{np}. The solid line is from the one-term Gaussian given in the text, the dotted line is from a Hulthén potential, and the dashed line is from a soft-core sum of Gaussians. Each of these V_{np}'s yields the same (S-wave) deuteron binding energy.

APPENDIX

The expansion of ψ_M via (1.4) is analogous to defining ψ_M as the solution of a single Lippmann-Schwinger (LS) equation. This has led to occasional comments that such an expansion cannot be valid, since a triad of LS equations, and not merely one, is required to define a unique solution for three-body problems.[33] While this latter point is valid in general, there is one circumstance when a triad is not needed and, as we show below, the present model is an instance of this latter situation.

In addition to the inhomogeneous LS equation, homogeneous ones are needed (to specify a unique solution) whenever rearrangements can occur. In the typical three-particle problem, two rearrangement channels exist and so a total of three LS equations are required.[33] We now recall a few theoretical aspects of this situation.[34] Let α, β, and γ denote the three two-body channels in this case, and let $\Phi_{\alpha,E}$, $\Phi_{\beta,E}$, and $\Phi_{\gamma,E}$ be "plane wave" states of total energy E in channels α, β, and γ. These states are given as a product of a bound state for the pair forming the channel times a plane wave for the third or spectator particle. The full scattering state that develops from any one of them, say from $\Phi_{\alpha,E}$, is denoted $\Psi_{\alpha,E}^{(+)}$. It is given by

$$\Psi_{\alpha,E}^{(+)} = \Omega_\alpha \Phi_{\alpha,E} , \qquad (A1)$$

where Ω_α is the relevant Møller operator.

Applying the adjoint operator $\Omega_\alpha^\dagger$ to both sides of (A1) yields

$$\Omega_\alpha^\dagger \Psi_{\alpha,E}^{(+)} = \Phi_{\alpha,E} , \qquad (A2)$$

which, as discussed in Ref. 34, is equivalent to the usual, inhomogeneous LS equation for $\Psi_{\alpha,E}^{(+)}$. However (A2) does not uniquely determine $\Psi_{\alpha,E}^{(+)}$ because of the relation $\Omega_\alpha^\dagger \Psi_{\beta,E}^{(+)} = 0$, $\beta \neq \alpha$. That is, $\Psi_{\alpha,E}^{(+)} + C_1 \Psi_{\beta,E}^{(+)}$ also satisfies (A2), where C_1 is an arbitrary constant and $\Psi_{\beta,E}^{(+)}$ obeys (A1) with β replacing α. In the typical situation $\Psi_{q,E}^{(+)} + C_2 \Psi_{\gamma,E}^{(+)}$ will also satisfy (A2) because of $\Omega_\alpha^\dagger \Psi_{\gamma,E}^{(+)} = 0$ (where C_2 is a second constant and $\Psi_{\gamma,E}^{(+)} = \Omega_\gamma \Phi_{\gamma,E}$). To avoid these admixtures, $\Psi_{\alpha,E}^{(+)}$ must obey a triad of one inhomogeneous and two homogeneous LS equations.[34]

In contrast to this, the H_M problem is an example of the atypical case in which no rearrangements can occur, i.e., the allowed processes for H_M are elastic scattering and elastic breakup but not (d,p) or (d,n) stripping. Stripping cannot occur because the absorptive optical potentials $\mathcal{V}_n(E_d/2)$ and $\mathcal{V}_p(E_d/2)$ cannot support particle-stable bound states. Consequently, for the "stripping channels" β and γ of this model, there are no plane wave states $\Phi_{\beta,E}$ or $\Phi_{\gamma,E}$, and therefore the corresponding full scattering states $\Psi_{\beta,E}^{(+)}$ and $\Psi_{\gamma,E}^{(+)}$ are zero. Thus, there can be no admixtures to the $\Psi_{\alpha,E}^{(+)}$ defined by a single, inhomogeneous LS equation describing elastic scattering and elastic breakup: it uniquely specifies a solution.

Even though a single LS equation defines a unique solution, this equation cannot be straightforwardly solved to yield that solution. The reason is that the kernel of the equation is not compact. The same is true when one works with the triad of LS equations: neither the single LS equation in this case nor the triad in the case of rearrangements allow numerical solutions to be obtained using the standard methods as employed in nuclear physics. If one wanted to use such methods in an integral equation approach, then a set like the Faddeev equations are required. A noncompact integral equation method such as that of the Iowa–Los Alamos Collaboration might be successful here,[35] although it has not yet been tested above the breakup threshold. However, one *can* use the single LS equation in the present case and the triad in the more general case to specify the asymptotic boundary conditions which must be imposed on the solution to the relevant Schrödinger equation. The physical statement of the boundary conditions for the H_M model is that only elastic scattering and breakup occur in the asymptotic region. A mathematical statement, combining the two physical processes, is given as Eq. (3.6). Imposing this form will yield a unique solution to the Schrödinger equation in the present case. That it failed to provide a complete set of stable FEM amplitudes for both models studied here has been explained above.

Notice that our argument relies crucially on the fact that the optical potentials are being evaluated at $E_d/2$— or at least on their not being energy dependent. On the other hand, with an energy dependence such as in Eq. (1.2), the model changes drastically. For example, we can have stripping at spectator-nucleon kinetic energies corresponding to capture of the stripped nucleon into those single particle states associated with the ground state of the target. At such energies, $\mathcal{V}_n^{opt}(E - \epsilon_0 - K_p)$, for example, becomes $\mathcal{V}_n^{opt}(E_{s.p.}^{(i)})$, with $E_{s.p.}^{(i)} \leq 0$, and according to Feshbach's original analysis,[36] $\mathcal{V}_n^{opt}(-|E_{s.p.}^{(i)}|)$ becomes real and thus capable of supporting the bound states corresponding to stripping. With the energy dependence of (1.2) thus retained, H_3 defines an energy-dependent, three-body model incorporating rearrangement and necessitating a Faddeev-like description. Because such a model is very nontrivial to analyze, we did not emphasize this aspect of H_3 in our earlier work. We believe that there are simpler three-body models for treating the coupled set of elastic processes (d,d), (d,p), (d,n), and (d,np), and will report on the results of our investigations of this problem in a future publication.

*Present address: Theoretical Division, Los Alamos National Laboratory, Los Alamos, NM 87545.

[1]See, e.g., H. Amakawa and N. Austern, Phys. Rev. C **27**, 922 (1983), and references cited therein.

[2]R. Kozack and F. S. Levin, Phys. Rev. C **34**, 1511 (1986).

[3]N. Austern and K. C. Richards, Ann. Phys. (N.Y.) **49**, 309 (1968).

[4]Such Pauli blocking terms had been conjectured to arise because of the analogy between the deuteron-nucleus collision problem and the description of the pair wave function in Bethe-Goldstone theory. Reference 2 contains a discussion of this point and references to the pertinent literature.

[5]M. Kawai and M. Yahiro, private communication.

[6]L. D. Faddeev, Zh. Eksp. Teor. Fiz. **39**, 1459 (1960) [Sov. Phys.—JETP **12**, 1014 (1961)]. For references to applications and theoretical developments, see, e.g., W. Glöckle, *The Quantum-Mechanical Few-Body Problem* (Springer, New York, 1983).

[7]S. Watanabe, Nucl. Phys. **8**, 484 (1958).

[8]R. C. Johnson and P. J. R. Soper, Phys. Rev. C **1**, 976 (1970); J. D. Harvey and R. C. Johnson, *ibid.* **3**, 636 (1971).

[9]H. Amakawa, A. Mori, H. Nishioka, K. Yazaki, and S. Yamaji, Phys. Rev. C **23**, 583 (1981).

[10]B. Anders and A. Linder, Nucl. Phys. **A296**, 77 (1978); M. Kawai, M. Kamimura, and K. Takesako, in Proceedings of 1978 INS International Symposium, Fukuoka (unpublished), p. 710.

[11]J. P. Farrell, C. M. Vincent, and N. Austern, Ann. Phys. (N.Y.) **96**, 333 (1976); N. Austern, C. M. Vincent, and J. P. Farrell, *ibid.* **114**, 93 (1978).

[12]G. H. Rawitscher, Phys. Rev. C **9**, 2210 (1974).

[13]M. Yahiro, M. Nakano, Y. Iseri, and M. Kamimura, Prog. Theor. Phys. **67**, 1467 (1982).

[14]G. Strang and G. Fix, *An Analysis of the Finite Element Method* (Prentice-Hall, New Jersey, 1973); K. Bathe and E. Wilson, *Numerical Methods in Finite Element Analysis* (Prentice-Hall, New Jersey, 1976); T. J. Chung, *Finite Element Analysis in Fluid Dynamics* (McGraw-Hill, New York, 1978).

[15]P. M. Prenter, *Splines and Variational Methods* (Wiley, New York, 1975).

[16]C. Gignoux, A. Laverne, and S. P. Merkuriev, Phys. Rev. Lett. **33**, 1350 (1974); S. P. Merkuriev, C. Gignoux, and A. Laverne, Ann. Phys. (N.Y.) **99**, 30 (1976).

[17]G. L. Payne, J. L. Friar, and B. F. Gibson, Phys. Rev. C **26**, 1385 (1983); C. R. Chen, G. L. Payne, J. L. Friar, and B. F. Gibson, *ibid.* **33**, 1740 (1986), and references therein.

[18]A. Askar and M. Demiralp, J. Chem. Phys. **60**, 2762 (1974);

G. D. Barg and A. Askar, Chem. Phys. Lett. **76**, 609 (1980), plus additional references cited therein to the work of Askar and his collaborators.

[19]M. Friedman, Y. Rosenfeld, A. Rabinovitch, and R. Thieberger, J. Comput. Phys. **26**, 169 (1978); A. Rabinovitch, R. Thieberger, and M. Friedman, J. Phys. B **18**, 393 (1985), plus additional references cited therein to the work of Thieberger, Friedman, and collaborators.

[20]C. Bottcher, J. Phys. B **14**, 349 (1981); **15**, 463 (1982).

[21]W. K. Ford and F. S. Levin, Phys. Rev. A **29**, 43 (1984); F. S. Levin and J. Shertzer, *ibid.* **32**, 3285 (1985).

[22]The Riccati modifications are discussed in Sec. 10 of the *Handbook of Mathematical Functions*, edited by M. Abramowitz and I. Stegun (Dover, New York, 1965).

[23]R. Kozack, Ph.D. thesis, Brown University, 1984 (unpublished).

[24]J. Revai and J. Raynal, Lett. Nuovo Cimento **9**, 461 (1974).

[25]Y. Yamaguchi, Phys. Rev. **95**, 1628 (1954).

[26]G. L. Payne, private communication.

[27]Some suggestions of possible instability are noted in Refs. 16 also.

[28]J. Nuttall, Phys. Rev. Lett. **19**, 473 (1967); J. Nuttall and J. G. Webb, Phys. Rev. **178**, 2226 (1969); J. Nuttall, J. Math. Phys. **12**, 1896 (1971); W. Glöckle, Z. Phys. **271**, 31 (1974).

[29]See, e.g., A. Erdelyi, *Asymptotic Expansions* (Dover, New York, 1957).

[30]Z. C. Kuruoglu and F. S. Levin, Phys. Rev. C **36**, 49 (1987).

[31]W. Glöckle, private communication.

[32]See, e.g., H. P. Noyes and H. Fiedeldey, in *Three-Particle Scattering in Quantum Mechanics*, edited by J. Gillespie and J. Nuttall (Benjamin, New York, 1968), pp. 201–209; H. P. Noyes, in *Three Body Problem in Nuclear and Particle Physics*, edited by J. S. C. McKee and P. M. Rolph (North-Holland, Amsterdam, 1970), pp. 13–16.

[33]For discussions concerning the triad, see F. S. Levin and W. Sandhas, Phys. Rev. C **29**, 1617 (1984), and references cited therein, as well as P. Benoist-Gueutal, *ibid.* **33**, 412 (1986), in addition to the comments on this article by F. S. Levin and W. Sandhas, *ibid.* **34**, 1140 (1986); E. Gerjuoy, *ibid.* **34**, 1143 (1986).

[34]A fuller discussion, on which our brief review is based, is given by W. Sandhas, in *Few Body Nuclear Physics* (IAEA, Vienna, 1978), p. 3.

[35]G. L. Payne, W. H. Klink, W. N. Polyzou, J. L. Friar, and B. F. Gibson, Phys. Rev. C **30**, 1132 (1984); W. N. Polyzou, W. H. Klink, and G. L. Payne, *ibid.* **30**, 1140 (1984).

[36]H. Feshbach, Ann. Phys. (N.Y.) **5**, 287 (1957).